

Quasi-continuous-wave diode-pumped Yb:YCOB monolithic laser with peak power beyond 200 W

Ya Zhou (周 亚), Fei Liang (梁 飞), Huichen Si (司会晨), Dazhi Lu (路大治), Haohai Yu (于浩海)**, and Huaijin Zhang (张怀金)

State Key Laboratory of Crystal Materials and Institute of Crystal Materials, Shandong University, Jinan 250100, China

*Corresponding author: liangfei@sdu.edu.cn

**Corresponding author: haohaiyu@sdu.edu.cn

Received November 20, 2024 | Accepted December 25, 2024 | Posted Online May 16, 2025

High-power diode-pumped solid-state lasers (DPSSLs) can support many important applications owing to their simple setup and high efficiency. However, the thermal effect in the laser crystal is a major limiting factor for laser power improvement. Here, we originally present a quasi-continuous-wave (QCW) diode-pumped monolithic Yb³⁺-doped YCa₄O(BO₃)₃ (Yb:YCOB) laser and realize the power scaling at room temperature by removing the heat efficiently. The Yb:YCOB laser at 1024 nm is designed with a quantum efficiency of 95%. A high-power QCW laser is realized with an output peak power of up to 226.7 W, a pulse energy of 12.2 mJ, and an optical-to-optical efficiency of 41.2%. To the best of our knowledge, this result represents the record peak power in Yb:YCOB lasers and should have promising applications in some modern devices requiring high-power and large-energy lasers.

Keywords: Yb:YCOB crystal; quasi-continuous wave; electron-phonon coupling.

DOI: [10.3788/COL202523.061403](https://doi.org/10.3788/COL202523.061403)

1. Introduction

High-power solid-state lasers have significant applications in many fields, such as industrial processing, national defense, and scientific research^[1–4]. Improving the output power with low cost is an enduring pursuit in the solid-state laser community. At present, ytterbium (Yb³⁺) ion-doped laser crystals are the commercialized gain media for near-infrared 1 μm laser generation^[5], e.g., Yb:YAG, Yb:YLF, and Yb:Lu₂O₃, owing to their low quantum defect, high thermal conductivity, and excellent power-scaling capacity. However, the Yb³⁺ ion is a quasi-three-level system, and its laser low level originates from the Stark-splitting of the ground state ²F_{7/2}. According to the Boltzmann distribution, the population at the low level is easily affected by the crystal temperature, thus resulting in a strong reabsorption effect and depressed lasing gain. In addition, the thermal lens effect^[6] usually results in the deterioration of beam quality and power attenuation. Therefore, high-power Yb³⁺ laser systems usually need strict thermal management to remove heat and improve the output power^[7,8].

To address the thermal effect of Yb-doped laser crystals, some advanced laser technologies have been developed, including thin-disk lasers, liquid-nitrogen (LN₂) refrigeration, liquid-helium (LH₂) refrigeration, and so on. For example, in 2009, a thin-disk laser setup of a continuous-wave (CW) laser operation with a Yb³⁺-doped YCa₄O(BO₃)₃ (Yb:YCOB) crystal

reached 26 W of output power at an optical-to-optical efficiency of 58%^[9]. Then, in 2010, a CW thin-disk laser was reported in a Yb:YCOB crystal with 101 W output power and 40% optical-to-optical conversion efficiency^[10]. In 2024, using a LN₂ dewar, a high-power Yb:YLF laser at 1019 nm was realized with 330 W output power and a slope efficiency of 69%^[11]. In addition, a similar result was reported in LN₂-cryogenic Yb:YAG lasers at 1030 nm with an output power of 140 W and a slope efficiency of 59%^[11]. Moreover, liquid-helium cooling can produce a lower temperature than LN₂-cooling and improve heat dissipation. In 2023, a Yb:YGG laser at 1022 nm was achieved in a helium cryostat with an output power of 18 W^[12]. Then, a LH₂-cryogenic Yb:YCOB laser at 1027 nm was realized with an output power of 7.91 W and a slope efficiency of 77.7%^[13]. As a result, these thermal management methods are very effective for removing heat during laser operation and make great power scaling in Yb-doped laser crystals. Nevertheless, the experimental setup of the thin-disk laser is quite complicated and time-consuming. The experimental setup of the cryogenic laser is unstable, which results in high cost and inconvenience. Therefore, some new thermal management techniques need to be developed with a simple setup and high integration.

According to the principle of heat conduction, reducing the heat accumulation in a laser crystal is beneficial for power scaling. This is mainly determined by the duration of the incident pump light. With the development of semiconductor diode

lasers, electrically modulated quasi-continuous-wave (QCW) diodes have been applied in solid-state laser systems^[14–17]. By changing the duty cycle of the pump pulse, QCW pumping can effectively reduce heat accumulation and improve the output power of diode-pumped solid-state lasers (DPSSLs). This method requires neither additional crystal welding nor a complex cooling chamber, which is favorable for the design of the miniaturized laser system. For example, in 2019, a QCW-pumped Yb:YAG laser at 1030 nm was reported with a peak power of 22.57 W^[18]. However, in the 940-nm-LD pumped Yb:YAG laser, its quantum defect was slightly larger, and the overall optical-to-optical conversion efficiency was only 16%. Accordingly, a highly-efficient and high-power QCW laser can be expected in other Yb-doped crystals with higher absorption coefficients and smaller quantum defects.

In this Letter, we employ a Yb:YCOB crystal as a gain medium, which has a large absorption cross section at 976 nm ($\sigma_{\text{abs}} = 1.05 \times 10^{-20} \text{ cm}^2$) and a large emission cross section at 1.02 μm ($\sigma_{\text{em}} = 0.39 \times 10^{-20} \text{ cm}^2$)^[19,20]. Compared to the Yb:YAG, the quantum defect of Yb:YCOB was reduced by 50.6%. Therefore, it is a promising gain medium for high-power scaling by QCW-pumping technology. To the best of our knowledge, such QCW lasers have never been realized in Yb:YCOB crystals. Here, via a rational cavity design, we presented a monolithic QCW Yb:YCOB laser at 1.02 μm with a peak power of 226.7 W, a pulse energy of 12.2 mJ, and an optical-to-optical efficiency of 41.2%. Meanwhile, the beam quality and power stability of the QCW laser were measured.

2. Results and Discussion

The QCW pumping source works at a certain duty cycle. When the crystal temperature rises to a certain value, it enters the heat dissipation stage without a pump light in each pulse period. The analytical expression of the transient temperature field of a laser crystal pumped by the end face of a QCW diode is given by^[21,22]

$$u(r, t) = \frac{2\alpha\eta ER}{k\pi w\tau_{\text{on}}} \sum_{m=1}^{\infty} \frac{J_0(\mu_m r/R) J_1(\mu_m w/R) f(p, t, \mu_m)}{\mu_m^3 J_1^2(\mu_m)}, \quad (1)$$

where u is the time-dependent temperature profile, r is the crystal length, t is the time, k is the thermal conductivity of the laser crystal, τ_{on} is the turn-on time, E is the pulse energy, R is the crystal radius, and w is the radius of the incident pump light. α is the absorption coefficient of the crystal, and the heat load efficiency of lasing is 0.32 (η). J_0 is the zeroth-order Bessel function. For the QCW Yb:YCOB laser, r is 6 mm, k is $2.3 \text{ W} \cdot \text{m}^{-1} \cdot \text{K}^{-1}$, R is 1.5 mm, w is 220 μm , and α is 2.7 cm^{-1} .

The transient temperature distributions at the center point of the front face of the Yb:YCOB crystal are shown in Fig. 1(a). At an incident peak power of 550 W, we set a fixed pulse width (τ) of 80 μs and pulse repetition frequencies (PRFs) of 100, 200, and 300 Hz, i.e., duty cycles of 0.8%, 1.6%, and 2.4%, respectively. It is obvious that when the pump pulse is 80 μs , the higher the PRF, the higher the residual temperature left by

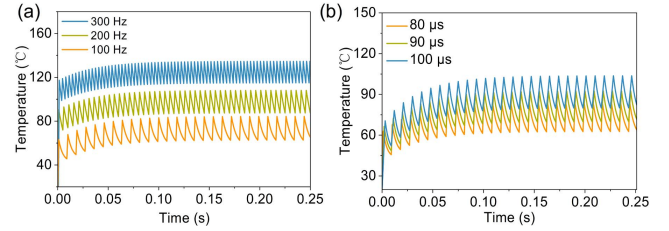


Fig. 1. (a) Transient temperature change of the Yb:YCOB front-face center at different PRFs with a pulse width of 80 μs . (b) The transient temperature change of the Yb:YCOB front-face center at different pulse widths with a PRF of 100 Hz.

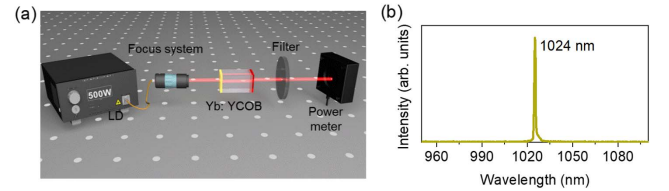


Fig. 2. (a) Experimental configuration of the QCW laser. (b) Laser spectrum of the QCW pumped laser.

the last pulse will be. Therefore, when the frequency is set as 300 Hz, the temperature of the Yb:YCOB crystal ($T = 114^\circ\text{C}$) is higher than 200 Hz ($T = 87^\circ\text{C}$) and 100 Hz ($T = 62^\circ\text{C}$) ultimately. In addition, the temperature distributions of the Yb:YCOB front face is dependent on the pulse width. Figure 1(b) depicts the transient temperature distributions at an incident peak power of 550 W, a fixed PRF of 100 Hz, and $\tau = 80, 90,$ and $100 \mu\text{s}$, respectively. It can be concluded that the temperature fluctuation amplitude in the crystal is mainly determined by the pulse width, and the time to reach the equilibrium temperature at 100 μs is longer than that at 80 and 90 μs . At the time of 0.25 s, the temperature of the three pulse widths gradually tends to balance, and the temperatures of $\tau = 80, 90,$ and $100 \mu\text{s}$ are $62^\circ\text{C}, 69^\circ\text{C},$ and 80°C , respectively. Therefore, the final temperature rise inside the Yb:YCOB crystal is determined by the duty cycle, and a low duty cycle is beneficial for reducing crystal temperature.

The experimental setup of the QCW laser is shown in Fig. 2(a). The pump source was a fiber-coupled diode laser with a center wavelength of 976 nm. The fiber diameter was 220 μm and the numerical aperture (NA) was 0.22. The pump light was focused on the laser crystal by a coupling lens system with a beam amplification ratio of 1:2. A 15% (atomic fraction) Yb³⁺-doped YCOB crystal was utilized in the laser experiments, cut along the x -axis (x -cut), y -axis (y -cut), and z -axis (z -cut). The crystal dimensions were 3 mm \times 3 mm \times 6 mm and 3 mm \times 3 mm front/end faces were polished and coated. In our setup, a plane–plane monolithic cavity was applied in the Yb:YCOB laser. Both the input mirror and the output coupler were coated on the front and end faces of the Yb:YCOB crystal directly. The input mirror was coated with high transmission (HT, $T > 95\%$) at 970–980 nm and high reflection (HR,

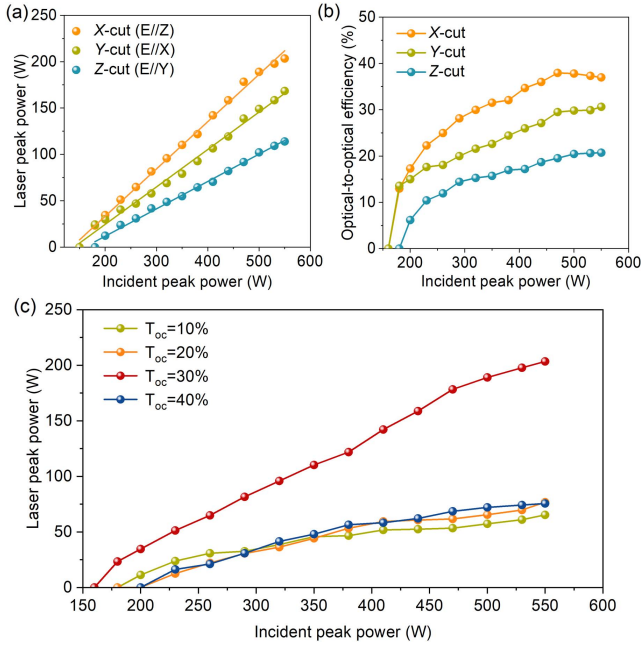


Fig. 3. (a) Output powers of the Yb:YCOB laser at 100 Hz, 90 μ s in the *x*-cut, *y*-cut, and *z*-cut crystals. (b) Optical-to-optical efficiency at 100 Hz, 90 μ s. (c) Laser peak powers in the *x*-cut crystal with various T_{oc} .

$R > 99.9\%$) at 1000–1200 nm. The output mirror was HT-coated with a certain transmittance ($T_{oc} = 30\%$) at 1020–1030 nm. To remove the waste heat in the laser operation, the Yb:YCOB crystal was mounted onto a copper block. The water-cooling temperature was set as 2°C. A filter was placed behind the Yb:YCOB crystal, which was HR-coated at 976 nm to reflect the residual pump light and HT-coated at 1000–1100 nm.

As shown in Figs. 3(a) and 3(b), the output powers of Yb:YCOB laser were measured in *x*-cut, *y*-cut, and *z*-cut crystals, respectively, with the PRF = 100 Hz and $\tau = 90 \mu$ s. The highest peak power and the highest conversion efficiency were obtained in the *x*-cut crystal. The maximum peak power was 203.4 W, and the optical-to-optical conversion efficiency was 36.99%. In comparison, the maximum powers in the *y*-cut and *z*-cut Yb:YCOB were 168.42 and 113.95 W, respectively, which was smaller than that of the *x*-cut crystal. This could be attributed to the spectral anisotropy of Yb:YCOB crystal. According to spectral analysis, the *x*-cut crystal allows the laser operation with $E\parallel Z$ polarization, which has the largest emission cross section of around 1.02 μ m among the three principal-axis directions^[23]. In order to evaluate the optimal transmittance of the output mirrors, we measured four different output couplers with $T_{oc} = 10\%$, 20%, 30%, and 40%, respectively, see Fig. 3(c). The *x*-cut Yb:YCOB crystal was used. When the incident peak power was 550 W, the output power gradually increased from 65.3, 76.7, to 203.4 W, with the transmission increasing from 10% to 30%, respectively. For the higher $T_{oc} = 40\%$, the output power dropped to 75.6 W. Therefore, $T_{oc} = 30\%$ should be an optimal transmittance for power scaling.

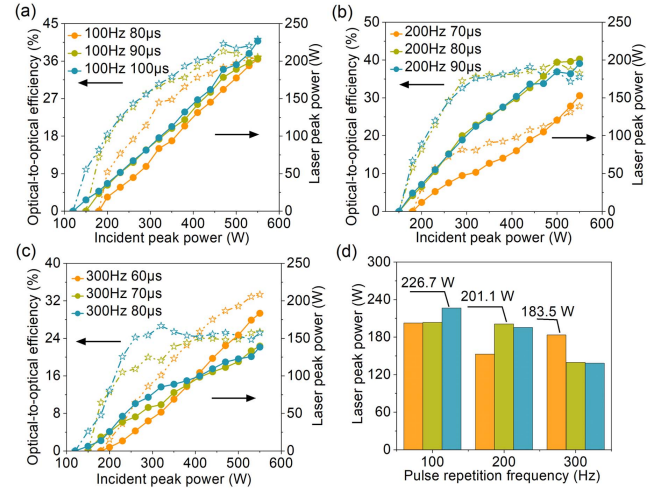


Fig. 4. Optical-to-optical efficiency and laser peak power of the Yb:YCOB laser at different PRFs. (a) 100 Hz, (b) 200 Hz, and (c) 300 Hz. (d) Comparison of the QCW Yb:YCOB laser peak powers of different PRFs and pulse widths.

Figures 4(a)–4(c) depict the output power and conversion efficiency at different duty cycles in the *x*-cut Yb:YCOB crystal ($T_{oc} = 30\%$). It could be seen that the maximum peak power and efficiency were obtained with the PRF = 100 Hz and $\tau = 100 \mu$ s. The highest peak power was 226.7 W, and the maximum optical-to-optical efficiency was 41.2%. The corresponding wavelength was 1.02 μ m, as shown in Fig. 2(b). At this time, the average output power was 1.23 W, and the single pulse energy was 12.24 mJ.

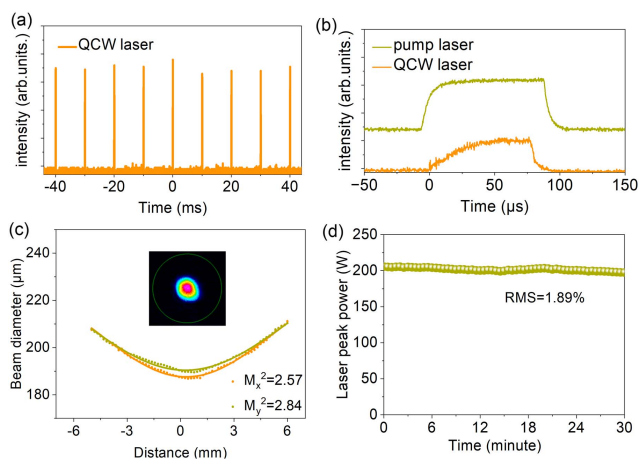
For the PRF = 200 Hz and the $\tau = 80 \mu$ s, the peak power and optical-to-optical conversion efficiency were 187.5 W and 34.1%, respectively. At this time, the average output power was 1.4 W, and the single pulse energy was 6.8 mJ. For the PRF = 300 Hz and for $\tau = 60 \mu$ s, the peak power was 183.5 W with an optical-to-optical conversion efficiency of 33.3%. At this time, the average output power was 1 W, and the single pulse energy was 3.33 mJ. The laser efficiency could be further improved by optimizing the mode matching in the cavity.

Figure 4(d) displays the comparison of the peak powers among different pulse widths and PRFs. It is observed that the peak power at 100 Hz is higher than that at 200 and 300 Hz, respectively. This can be attributed to the effective heat dissipation during low repetition frequency. At a low PRF, the heat generated by each pulse can be dissipated in time at the process of QCW pumping. With the increasing PRFs, the heat dissipation is not timely enough, which makes it easy to produce the gradual accumulation of heat, thereby reducing the output power and lasing efficiency.

In Table 1, we make a comprehensive comparison for the QCW end-pumped monolithic laser in Yb³⁺-doped materials. In previous studies^[18,24–31], QCW-pumped lasers at 1 μ m have been realized in garnet Yb:YAG, Yb:LuYAG, Yb:GdYAG, Yb:YSAG, sesquioxide Yb:(Lu,Y)₂O₃, Yb:Lu₂O₃, silicate Yb:SSO, and fluoride Yb:CaF₂. Among them, Yb:GdYAG exhibited the highest peak power of 39 W at 1030 nm. The Yb:SSO crystal laser was reported at a long wavelength of 1036 nm, with a slightly larger quantum loss and a reduced peak power of 27.6 W.

Table 1. Comparison of QCW End-Pumped Monolithic Lasers in Yb³⁺-Doped Ceramics/Crystals.

Crystal	Pump wavelength (nm)	Laser wavelength (nm)	Peak power (W)	Ref.
Yb:YAG	940	1030	22.57	[18]
Yb:CaF ₂	930	1028.9	5.6	[24]
Yb:YAG	936	1030	26.5	[25]
Yb:LuYAG	936	1030	36.5	[26]
Yb:GdYAG	930	1030.55	39	[27]
Yb:YSAG	936	1031	31.5	[28]
Yb:(Lu,Y) ₂ O ₃	936	1032	17	[29]
Yb:Lu ₂ O ₃	930	1033.3	14.4	[30]
Yb:SSO	976	1036&1062	27.6	[31]
Yb:YCOB	976	1024	226.67	This work

**Fig. 5.** (a) Pulse train of the QCW laser at 100 Hz, 100 μ s. (b) The single pulse profiles of the pump laser and the Yb:YCOB laser at 100 Hz, 100 μ s. (c) Beam profile and beam quality of the Yb:YCOB laser with a peak power of 205.5 W. (d) Power stability of the Yb:YCOB laser.

In comparison, our reported Yb:YCOB laser wavelength was 1024 nm, which held a lower quantum defect than the Yb:GdYAG and the Yb:SSO. As a result, the Yb:YCOB has a high peak power of 226.7 W, surpassing all reported QCW end-pumped Yb³⁺-doped monolithic lasers around 1 μ m. This case suggests that there is potential in Yb:YCOB and other laser crystals with low quantum defect to realize power scaling by QCW-pumping. Referring to the Yb:YAG slab laser^[16], the power and efficiency of the QCW-pumped Yb:YCOB laser could be further improved by applying a slab gain medium.

Finally, we measured the temporal characteristics, beam quality, and power stability of the QCW-pumped Yb:YCOB laser. As shown in Fig. 5(a), the Yb:YCOB laser was a typical pulse

laser with a PRF of 100 Hz. The output pulse of the QCW laser was very stable, and there was no frequency drift between pulses. The single pulse profile was monitored by an oscilloscope and displayed in Fig. 5(b). The pulse width of the Yb:YCOB laser was 60 μ s, which was less than the pump pulse (100 μ s), owing to the buildup time of the laser oscillation^[32]. As shown in Fig. 5(c), the measured values of M_x^2 and M_y^2 are 2.57 and 2.84 along the x -axis and y -axis, respectively. At this time, the output peak power was 205.5 W. The inset graph showed the two-dimensional beam intensity profile, which had a near-Gaussian spatial mode. The power stability of the laser was characterized by recording the fluctuation of the output power over 30 min. As depicted in Fig. 5(d), the root-mean-square (RMS) value of the output power was 1.89%, suggesting that this QCW-pumped Yb:YCOB laser was very stable.

3. Conclusion

In summary, we obtained a high-power QCW-pumped Yb:YCOB monolithic laser at 1024 nm with a peak power of 226.7 W. This work displays that the technology of QCW-pumping could effectively reduce the thermal effect in laser crystals, thereby realizing high power, good beam quality, and excellent power stability. Based on this high-power 1.02- μ m laser, an efficient green laser at 0.51 μ m can be designed by a highly integrated nonlinear frequency conversion, which could be applied in copper welding and laser processing.

Acknowledgements

This work was supported by the National Key Research and Development Program of China (Nos. 2021YFA0717800, 2021YFB3601504, and 2023YFF0718801), the National Natural Science Foundation of China (Nos. 52025021, 52422201, 52372010, and U23A20558), the Natural Science Foundation of Shandong Province (No. ZR2023ZD53), and the Future Plans of Young Scholars at Shandong University.

References

1. Y. Qi, S. Zhang, Z. Ye, *et al.*, "Multi-mode stable, high peak power Nd:YAG laser device for laser cleaning," *Appl. Opt.* **63**, 3277 (2024).
2. O. Kalisky, "The status of high-power lasers and their applications in the battlefield," *Opt. Eng.* **49**, 091003 (2010).
3. Y. Kawahito, H. Wang, S. Katayama, *et al.*, "Ultra high power (100 kW) fiber laser welding of steel," *Opt. Lett.* **43**, 4667 (2018).
4. P. Shukla, J. Lawrence, and Y. Zhang, "Understanding laser beam brightness: A review and new prospective in material processing," *Opt. Laser Technol.* **75**, 40 (2015).
5. R. L. Byer, "Diode laser-pumped solid-state lasers," *Science* **239**, 742 (1988).
6. P. Shang, L. Bai, S. Wang, *et al.*, "Research progress on thermal effect of LD pumped solid state laser," *Opt. Laser Technol.* **157**, 108640 (2023).
7. L. D. DeLoach, S. A. Payne, L. L. Chase, *et al.*, "Evaluation of absorption and emission properties of Yb³⁺ doped crystals for laser applications," *IEEE J. Quantum Electron.* **29**, 1179 (1993).
8. F. D. Patel, E. C. Honea, J. Speth, *et al.*, "Laser demonstration of Yb₃Al₅O₁₂ (YbAG) and materials properties of highly doped Yb:YAG," *IEEE J. Quantum Electron.* **37**, 135 (2001).

9. C. Kränkel, R. Peters, K. Petermann, *et al.*, "Efficient continuous-wave thin disk laser operation of Yb:Ca₄YO(BO₃)₃ in E||Z and E||X orientations with 26 W output power," *J. Opt. Soc. Am. B* **26**, 1310 (2009).
10. O. H. Heckl, C. Kränkel, C. R. E. Baer, *et al.*, "Continuous-wave and modulated Yb:YCOB thin disk laser: first demonstration and future prospects," *Opt. Express* **18**, 19201 (2010).
11. M. Kilinc, U. Demirbas, J. Thesinga, *et al.*, "Fractional thermal load in cryogenically cooled Yb:YLF and Yb:YAG lasers," *Opt. Mater. Express* **14**, 1499 (2024).
12. S. Slimi, V. Jambunathan, G. Zin Elabedine, *et al.*, "Spectroscopic and lasing characteristics of Yb:YGG at cryogenic temperatures," *Opt. Laser. Technol.* **167**, 109713 (2023).
13. J. M. Serres, "Cryogenic continuous-wave microchip Yb:YCOB laser," in *7th International Conference on Optics, Photonics and Lasers* (2024), Vol. **41**, p. 108.
14. J. Cheng, X. Zhang, P. Zhang, *et al.*, "Comparison of QCW pulsed laser and single-mode CW laser on the welding of power cell lugs," *J. Laser Appl.* **33**, 032008 (2021).
15. H. W. Bruesselbach, D. S. Sumida, R. A. Reeder, *et al.*, "Low-heat high-power scaling using InGaAs-diode-pumped Yb:YAG lasers," *IEEE J. Sel. Top. Quantum Electron.* **3**, 105 (1997).
16. S. Meng, Z.-Z. Chen, Y. Bo, *et al.*, "6.2 kW quasi-continuous-wave diode-pumped Yb:YAG ceramic slab laser," *Laser Phys.* **30**, 015802 (2019).
17. C. Jia, H. Guo, Y. Yao, *et al.*, "High energy and high repetition rate QCW-LD end-pumped electro-optical Q-switched Yb:YAG laser," *Opt. Continuum* **3**, 778 (2024).
18. Y. Wang, P. Wang, Y. Chen, *et al.*, "Experiments and simulations of QCW Yb:YAG laser with consideration of transient temperature," *Opt. Commun.* **435**, 433 (2019).
19. F. Mougél, K. Dardenne, G. Aka, *et al.*, "Ytterbium-doped Ca₄GdO(BO₃)₃: an efficient infrared laser and self-frequency doubling crystal," *J. Opt. Soc. Am. B* **16**, 164 (1999).
20. D. Lu, Q. Fang, X. Yu, *et al.*, "Power scaling of the self-frequency-doubled quasi-two-level Yb:YCOB laser with a 30% slope efficiency," *Opt. Lett.* **44**, 5157 (2019).
21. E. H. Bernhardt, A. Forbes, C. Bollig, *et al.*, "Estimation of thermal fracture limits in quasi-continuous-wave end-pumped lasers through a time-dependent analytical model," *Opt. Express* **16**, 11115 (2008).
22. L. Li, J. Nie, X. Feng, *et al.*, "Transient temperature distribution of Nd:YAG rod end-pumped by quasi-continuous-wave laser diode," *Laser Optoelectron. P.* **47**, 091404 (2010).
23. P. Loiko, J. M. Serres, X. Mateos, *et al.*, "Thermal lensing and multiwatt microchip laser operation of Yb:YCOB crystals," *IEEE Photonics J.* **8**, 1 (2016).
24. L. Guo, Y. Shi, F. Tian, *et al.*, "Microstructure and laser performance of fine-grained Yb:CaF₂ transparent ceramics prepared by two-step sintering," *Opt. Mater.* **140**, 113841 (2023).
25. L. Esposito, J. Hostaša, A. Piancastelli, *et al.*, "Multilayered YAG-Yb:YAG ceramics: manufacture and laser performance," *J. Mater. Chem. C* **2**, 10138 (2014).
26. G. Toci, A. Pirri, J. Li, *et al.*, "First laser emission of Yb_{0.15}(Lu_{0.5}Y_{0.5})₃Al₅O₁₂ ceramics," *Opt. Express* **24**, 9611 (2016).
27. Y. Feng, Z. Liu, G. Toci, *et al.*, "Fabrication, microstructure, spectral properties, and laser performance of Yb:GdxY_{3-x}Al₅O₁₂ ceramics," *J. Am. Ceram. Soc.* **107**, 4134 (2024).
28. A. Pirri, G. Toci, J. Li, *et al.*, "A Comprehensive characterization of a 10 at.% Yb:YSAG laser ceramic sample," *Materials* **11**, 837 (2018).
29. G. Toci, A. Pirri, B. Patrizi, *et al.*, "High efficiency emission of a laser based on Yb-doped (Lu,Y)₂O₃ ceramic," *Opt. Mater.* **83**, 182 (2018).
30. Z. Liu, Y. Feng, G. Toci, *et al.*, "Influence of annealing on microstructures and properties of Yb:Lu₂O₃ transparent ceramics," *J. Am. Ceram. Soc.* **107**, 1974 (2024).
31. H. Jiang, L. Xu, X. Chen, *et al.*, "Experimental research on end-pumped quasi-continuous wave Yb:SSO laser," *Chin. J. Laser* **43**, 1101007 (2016).
32. Y. Chen, W. Liu, Y. Bo, *et al.*, "High-efficiency high-power QCW diode-side-pumped zigzag Nd:YAG ceramic slab laser," *Appl. Phys. B* **111**, 111 (2013).